Materials Science Forum Vols. 539-543 (2007) pp. 3795-3800
online at http://www.scientific.net

Residual Strain Measurements in a Friction-Stir Processed AZ31B Magnesium Alloy Using Neutron Diffraction

W. Woo[1,2,a], H. Choo[1,2,b*], D. W. Brown[3], B. Clausen[3], Z. Feng[2], and P. K. Liaw[1]

[1]Materials Science and Engineering Department, The University of Tennessee, Knoxville, TN 37996, USA
[2]Metals and Ceramics Division, Oak Ridge National Laboratory, Oak Ridge, TN 37831, USA
[3]Materials Science and Technology Division, Los Alamos National Laboratory, Los Alamos, NM 87545, USA

[a]wwoo@utk.edu, [b]*hchoo@utk.edu, Corresponding Author, Tel. +1 865 974-3643, Fax. +1 865 974-4115

Keywords: Residual strain, Friction-stir processing, Magnesium alloys, Neutron diffraction

Abstract

Residual strain profiles in friction-stir processed (FSP) AZ31B magnesium-alloy plates were measured using neutron diffraction. Two different specimens were prepared to investigate the influences of the tool shoulder and the tool pin on the residual-strain profiles: (*Case 1*) a plate processed with both the stirring pin and tool shoulder, i.e., a regular FSP plate subjected to both the plastic deformation and frictional heating, and (*Case 2*) a plate processed only with the tool shoulder, i.e., subjected mainly to the frictional heating. The results show that the strain profiles of both cases are qualitatively quite similar. The longitudinal strain is mainly tensile with its maximum near the bead of the FSP plate. On the other hand, the transverse and normal strains are mildly compressive in both *Cases 1* and *2*.

1. Introduction

Friction-stir welding (FSW) is a solid-state joining process that has many advantages over the traditional fusion-welding processes [1]. FSW uses a rotating tool consisting of a threaded pin and a tool shoulder to apply the severe plastic deformation and frictional heating to the base metal, which produce a strong metallurgical joint. The friction-stir processing (FSP), a variation of FSW, is applied to modify the material microstructure by localized grain size refinements and homogenization of precipitate particles [2]. For example, Ma *et al.* reported superplasticity in Al alloys subjected to grain size refinements via FSP [3].

Recently, the FSW/FSP has been applied to magnesium alloys [4-10], which is one of the lightest metals in use for structural applications. Examples of the studies on FSP-Mg include the investigation of the microstructural evolution of a wrought FSW AZ31B [4] and the heat-resistant FSW Mg-Al-Ca alloy [5]; and fabrication of highly-formable AZ91D plates via multi-pass FSP [6]. Moreover, a number of studies focused on the understanding of the influence of texture on the mechanical behavior of the FSW Mg alloy to address its poor workability at room temperature due to the limited number of slip systems available in the hexagonal close-packed (hcp) structure

[12,13]. For example, texture of the fractured surface in AZ61 [7], micro-texture evolutions in AZ61 [8], tensile properties of AZ31B-H24 [9], grain size/orientation of AZ31 [10], and texture effect on the tensile behavior of AZ31B [11] were investigated for the FSW Mg alloy.

The residual stresses induced by the frictional heating and plastic deformation during the processing can also be detrimental to the integrity and performance of the FSW/FSP components [14,15]. For example, Reynolds *et al.* reported maximum longitudinal residual stress approaching 100% of the yield strength (300 MPa) of the base material in a 304L stainless steel FSW [16]. In this paper, we present the residual strain profiles of a FSP AZ31B Mg alloy measured using the neutron-diffraction technique.

2. Experimental procedures

As-received commercial AZ31B magnesium-alloy plate (hot-rolled and soft-annealed) has the nominal chemical composition in weight percent of 3.0 Al, 1.0 Zn, 0.2 Mn, and balance Mg. The dimension of the FSP specimen was 306 x 306 x 6.5 mm, Fig. 1. The transverse sides of the plate were clamped using pressing bars to constrain the displacement of the specimen during processing and the clamping was removed after the plate was cooled to 25 °C. All samples were prepared by the "bead-on-plate" processing method using a single plate to eliminate the complication from the gap variations.

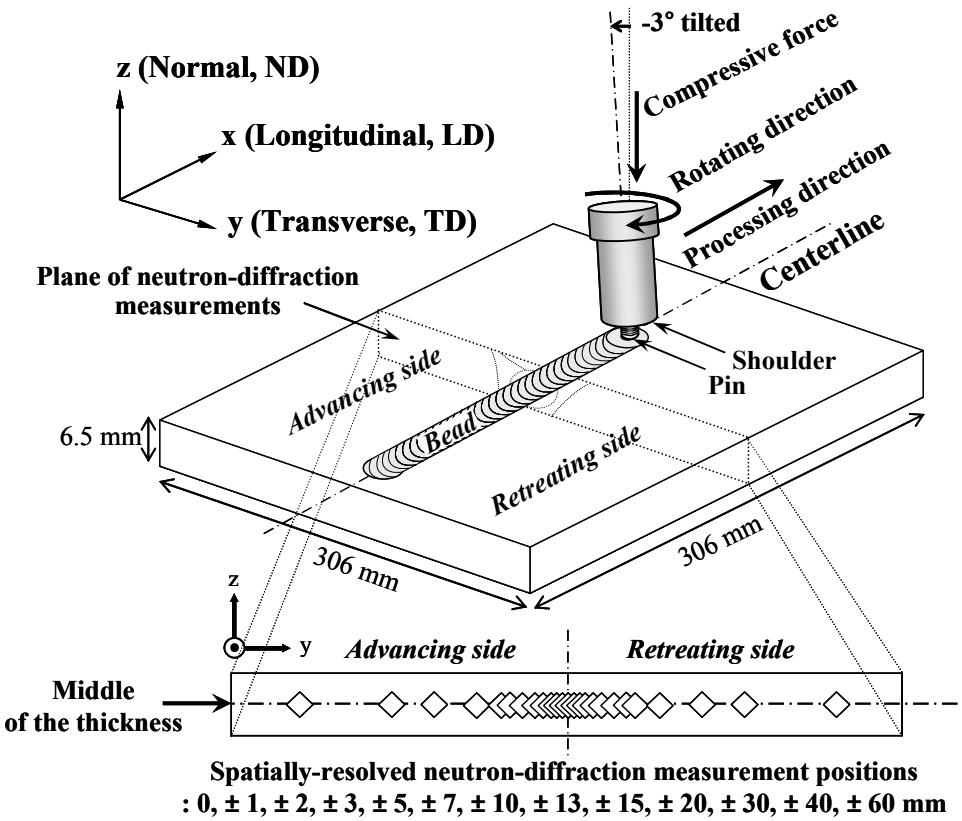

Fig. 1. Schematic of the friction-stir processing (FSP) and spatially-resolved neutron-diffraction measurement positions across the centerline of the FSP AZ31B Mg alloy plate.

The FSP plate was processed using a stirring pin and tool shoulder made of an H-13 tool steel. The plate was processed using the following parameters: 0.97 mm/sec traveling speed, 600 rpm clockwise rotating speed, and 12.4 MPa nominal compressive pressure using a tool with a 19.05-mm shoulder diameter and a 6.35-mm pin diameter with a 5.72-mm pin height. The tool was tilted 3 degrees opposite to the processing direction, which coincides with the rolling direction of the plate. Note that LD, TD, and ND denote longitudinal, transverse, and normal directions of the plate, Fig. 1.

Spatially-resolved neutron-diffraction measurements were performed to investigate the residual strain distributions [17]. The SMARTS (Spectrometer for MAterials Research at Temperature and Stress) instrument at the Los Alamos Neutron Science Center was used to determine the three principal strain components, i.e., longitudinal (ε_{xx}), transverse (ε_{yy}), and normal (ε_{zz}) strains [18]. The ε^{xx} and ε^{zz} components were measured simultaneously at the middle of the plate length (x) and thickness (z) along the y-direction using a 2 (x) × 2 (y) × 2 (z) mm scattering volume, Fig. 1. The ε^{yy} and ε^{zz} components were measured using a scattering volume of 20 (x) × 2 (y) × 2 (z) mm with the long dimension along the x-direction. Lattice parameters for both a- and c-axes of the hcp Mg alloy were obtained by the Rietveld refinement of the diffraction patterns using the General Structure Analysis System (GSAS) [19]. Residual strains were calculated using: $\varepsilon = (a - a_o) / a_o$, where a is the lattice spacing measured across the centerline and a_o is the "stress-free" lattice spacing measured at 60 mm away (on the advancing side) from the centerline for each scan setup. Note that the residual strains were determined along the a- and c-axes, i.e., ε_a and ε_c [20].

3. Results and discussion

3.1. Residual strains in Case 1

Figure 2 shows the three components of residual strains (i.e., ε^{xx}, ε^{yy}, and ε^{zz}) measured using neutron diffraction from the two different FSP plates. Note that the bead widths on the plate surface are approximately 20 mm and 18 mm in *Cases 1* and *2*, respectively. In *Case 1*, the three strain profiles show different characteristics, Figs. 2(a)-2(c). Overall, the ε^{xx} component shows significant tension, while the ε^{yy} and ε^{zz} components exhibit mild compression.

The ε^{xx} along the a-axis (ε_a^{xx}, i.e., strains in grains oriented with their a-axis parallel to the longitudinal direction) shows that the tensile residual strain increases up to about 1,800 x10^{-6} (or με) near the bead edges and drops to about 640 με near the centerline resulting in a valley shape in the profile within ±4 mm from the centerline of the plate. The ε_c^{xx} shows more fluctuations with a larger error bar (about 800 με). The large error bar in the ε_c^{xx} is due to the experimental uncertainties caused by the strong texture and the low intensities of the reflections from the basal planes along LD [11]. The discrepancy between ε_a^{xx} and ε_c^{xx} could be related to the plastically anisotropic properties between a- and c-axis at grains of the hcp Mg alloy, which may cause the intergranular strains arisen from strain mismatch between grains of different orientations [13]. The ε^{yy} and ε^{zz} components show relatively mild compressive residual strains, Figs. 2(b) and (c), except for the valley (large compressive strain) near the bead in the ε_a^{zz}. It should be noted here that ε_c^{yy}, Fig. 2(b), has a few missing data points within ±3 mm from the centerline due to the weak intensities of the basal plane along the TD in that region. Detailed texture results of the FSP Mg alloy will be reported in a future publication.

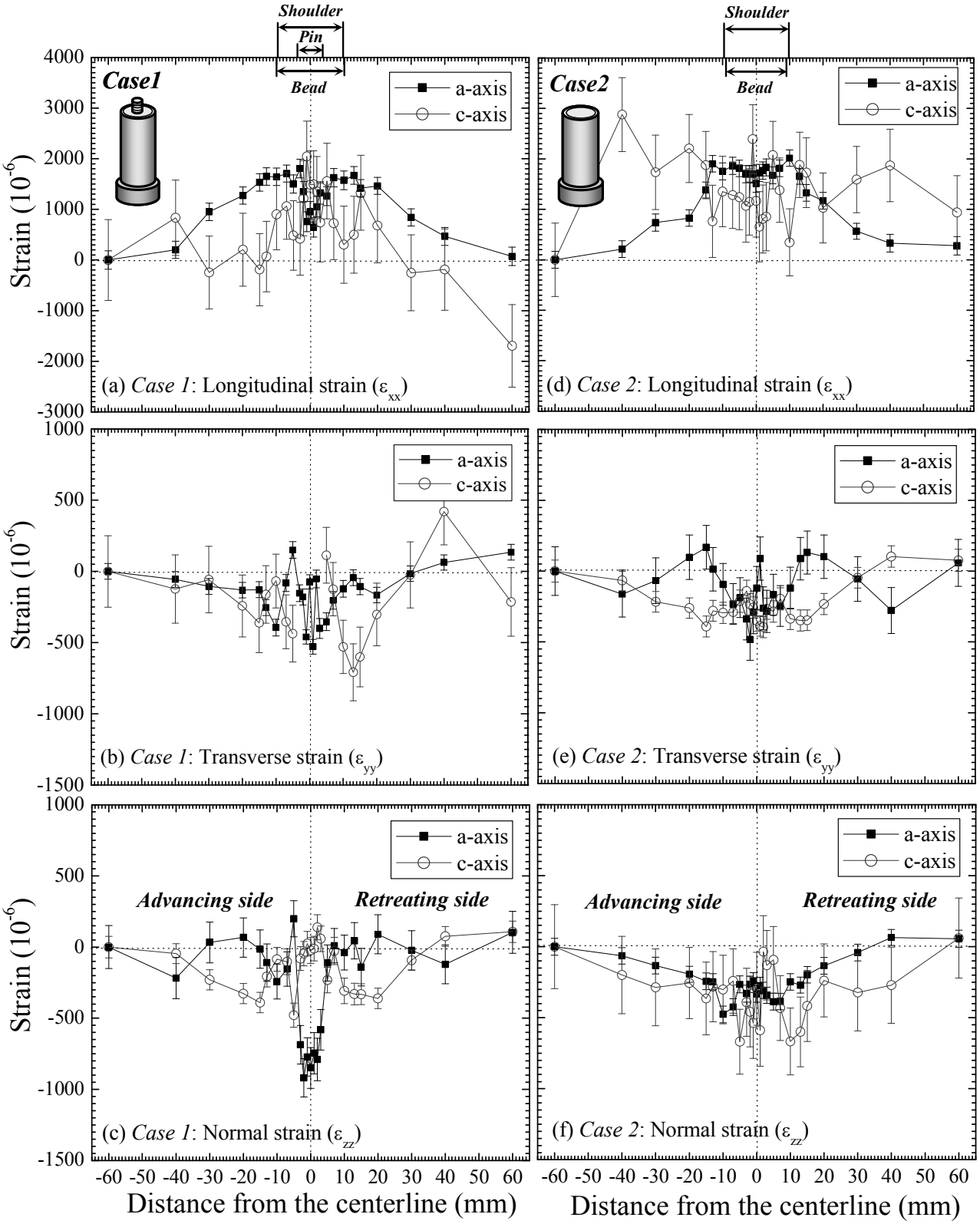

Fig. 2. Residual strain profiles measured across the centerline in the middle of the plate thickness: (a) Longitudinal (ε^{xx}), (b) transverse (ε^{yy}), and (c) normal (ε^{zz}) strains in *Case 1* (a typical FSP); (d) ε^{xx}, (e) ε^{yy}, and (f) ε^{zz} in *Case 2* (the shoulder-only case) as a function of the distance from the centerline. The tool design for *Cases 1* and *2* are shown in the insets.

3.2. Residual strains in Case 2

The shoulder-only case (*Case 2*), subjected mainly to the frictional heating during the FSP, is presented in Fig. 2(d)-2(f). Overall shape of the residual strain profiles in *Case 2* is similar to those of *Case 1*. For example, in *Case 2*, the ε_a^{xx} also shows its maximum tension (up to about 2,000 με) near the bead of the plate and the ε^{yy} and ε^{zz} components show relatively mild compression near the bead. However, compared to *Case 1*, there are two distinct characteristics in the strain profiles of *Case 2*. First, the ε_a^{xx} and ε_a^{zz} in *Case 2* do not show the noticeable valley shape, Figs. 2(d) and (f). Instead, the ε_a^{xx} in *Case 2*, Fig. 2(d), shows a plateau with a small fluctuation (between 1,530~2,000 με) within the bead. Comparing the diameter of the tool pin (6.35 mm) and the width of the valley (about 8 mm) in *Case 1*, the absence of the valley in *Case 2* seems to be related to the effect of the stirring tool pin. Secondly, the ε_c^{yy} in *Case 2*, Fig. 2(e), shows no missing data points within ±3 mm from the centerline unlike *Case 1* due to less significant texture variations in *Case 2*. As a result, ε_c^{yy} near the bead was measured with adequate statistics.

3.3. Characteristics of the residual strain profiles in FSP Mg alloy

First, tensile residual-strain profiles of *Cases 1* and *2* can be compared to the well-established results of the conventional fusion welding [14]. The overall shape of ε^{xx} along the a-axis, shown in Figs. 2(a) and 2(d), is similar to that of a typical arc weld in that extensive tensile distribution and its maximum located near the bead. Considering the a-axis of grains can comprise the majority of grains in the strongly textured Mg alloy, the ε^{xx} along the a-axis can represent the mechanical behavior of the bulk than the c-axis [20]. The similarity of the profiles between the FSP and fusion welding is attributed to the fact that ε^{xx} in both processes is generated due to the localized thermal expansion by the moving heat source under the restraint of the cold base materials during processing, followed by a hindered shrinkage during the subsequent cooling.

Secondly, the results of FSP Mg alloy are similar to those observed in FSP Al-6061 alloys. The previous results of the FSP Al-6061 alloy clearly showed the characteristic peak-and-valley shape and a wide valley region in the residual strain profiles near the bead [21]. The significant decrease of the residual strain near the centerline in the FSP Al-6061 alloy is related to the microstructural softening (e.g., the reduction of the yield strength and hardness) due to microstructure changes such as dissolution or aging of the precipitates and/or grain size changes [22]. Similarly, a narrow valley region within the bead is observed despite the relatively uniform microstructure in the FSP Mg alloy, e.g., the relatively uniform grain size and dislocation density throughout the plate [7]. More detailed microstructural studies are currently underway.

Finally, comparing ε_a^{xx} between *Cases 1* and *2*, the effect of the frictional heat on the residual strains can be discussed. The residual strain profile in *Case 2* is comparable to *Case 1* in terms of both the magnitude and profile shape except the valley near the centerline in *Case 1*. It implies that the frictional heating from the tool shoulder is the major source of residual strains in the FSP Mg alloy [21]. Schmidt *et al.* suggested that 86% of the heat during FSW 2024-T3 Al alloy is generated by the friction of the tool shoulder based on an analytical model [23]. Thus, when FSP is used to modify the surface microstructure of the wrought Mg alloy even without using the tool pin, it is expected that the materials have residual strains comparable to a typical FSW part.

4. Summary

Residual strains in a friction-stir processed (FSP) AZ31B magnesium-alloy plate were measured using neutron diffraction. Two different specimens were prepared with the purpose of comparing the effects of the tool pin and the shoulder on the residual strain distribution in the FSP Mg alloy plates: (*Case 1*) a plate processed with both stirring pin and tool shoulder, i.e., a regular FSP plate subjected to both plastic deformation and frictional heat, and (*Case 2*) a plate processed only with the tool shoulder, i.e., subjected mainly to the frictional heating. The results show that the longitudinal strain profiles are significantly tensile near the centerline of the plate, while the transverse and normal strain profiles are mildly compressive in both *Cases 1* and *2*. Furthermore, the comparison of the two cases shows that the heat input from the tool shoulder is a main source of the residual strains in the FSP Mg alloy.

Acknowledgements

This work is supported by the NSF International Materials Institutes (IMI) Program under contract DMR-0231320. This work has benefited from the use of the Los Alamos Neutron Science Center at the Los Alamos National Laboratory. This facility is funded by the US Department of Energy under Contract W-7405-ENG-36. The authors would like to thank A. Frederick and T. Sisneros for their help during experiments.

References

[1] M.W. Mahoney, C.G. Rhodes, J.G. Flintoff, R.A. Spurling, and W.H. Bingle: Mater. Trans. A Vol. 29 (1998), p. 1955
[2] P.B. Berbon, W.H. Bingel, R.S. Mishra, C.C. Bampton, and M.W. Mahoney: Scripta Mater. Vol. 44 (2001), p. 61
[3] Z.Y Ma, R.S. Mishra, and M.W. Mahoney: Acta Mater. Vol. 50 (2002), p. 4419
[4] J.A. Esparza, W.C. Davis, E.A. Trillo, and L.E. Murr: J. Mater. Sci. Lett. Vol. 21 (2002), P. 917
[5] D. Zhang, M. Suzuki, and K. Maruyama: Scripta Mater. Vol. 52 (2005), p. 899
[6] Y.S. Sato, S.H.C. Park, A. Matusunaga, and H. Kokawa: J. Mat. Sci. Vol. 40 (2005), p. 637
[7] S.H.C. Park, Y.S. Sato, and H. Kokawa: Scripta Mater. Vol. 49 (2003), p. 161
[8] S.H.C. Park, Y.S. Sato, and H. Kokawa: Metal. Mater. Trans. A Vol. 34 (2003), p. 987
[9] W.B. Lee, Y. M. Yeon, and S. B. Jung: Mater. Sci. Tech. Vol. 44 (2004), p. 785
[10] C.I. Chang, C.J. Lee, and J.C. Huang: Scripta Mater. Vol. 51 (2004), p. 509
[11] W. Woo, H. Choo, D.W. Brown, P.K. Liaw, and Z. Feng: Scripta Mater. Accepted
[12] ASM Speciality Handbook: *Magnesium and Magnesium Alloys* (Materials Park, Ohio: ASM international 1999)
[13] S.R. Agnew, C.N. Tomé CN, D.W. Brown, T.M. Holden, and S.C. Vogel: Scripta Mater. Vol. 48 (2003), p. 1003
[14] K. Masubuchi: *Analysis of Welded Structures* (Pergamon, New York 1980)
[15] P.J. Withers and H.K.D.H. Bhadeshia: Mater. Sci. Tech. Vol. 17 (2001), p. 366
[16] A.P. Reynolds, W. Tang, T.G. Herold, H. Prask, Scripta Mater. 48 (2003) 1289-1294.
[17] C.G. Windsor: *Pulsed Neutron Scattering* (Taylor and Francis, London 1981)
[18] M.A.M Bourke, D.C. Dunand, and E. Ustundag: Appl. Phys. A Vol. 74 (2002), p. S1707
[19] A.C. Larson and R.V. Von Dreele, *General Structure Analysis System (GSAS)* (Los Alamos National Laboratory Report 2004;LAUR 86-748)
[20] D.W. Brown, R. Varma, M.A.M. Bourke, T. Ely, T.M. Holden, and S. Spooner: ECRS 6: Sci. Forum Vol. 404-4 (2002), p. 741
[21] W. Woo, H. Choo, D.W. Brown, Z. Feng, P.K. Liaw, S.A. David, C.R. Hubbard, and M.A.M. Bourke: Appl. Phys. Lett. Vol. 86 (2005), p. 231902
[22] M. Peel, A. Steuwer, M. Preuss, and P.J. Withers: Acta Mater. Vol. 51 (2003), p. 4791
[23] H. Schmidt, J. Hattel, and J. Wert: Model. Simul. Mater. Sci. Eng. Vol. 12 (2004), p. 143.